OPEN ACCESS

ARTICLE

Discovery of S1P/SPHK1 dysregulation in Parkinson's disease and its role in pathological α-synuclein-induced neurodegeneration

Jiacheng Fang,[1,8] Xiaoxiao Wang,[1,8] Xiuli Su,[2] Dan Li,[1] Fuyue Wang,[1] Pengxi Wang,[3] Chenrui Yuan,[1] Fenfen Ji,[1] Doudou Zhang,[4] Xiaodong Cai,[4] Wenlan Liu,[5] Min Li,[6] Shen Hu,[7] and Zongwei Cai[1,2,*]

*Correspondence: zwcai@hkbu.edu.hk

Received: April 9, 2025; Accepted: October 13, 2025; Published Online: October 16, 2025; https://doi.org/10.59717/j.xinn-life.2025.100164

GRAPHICAL ABSTRACT

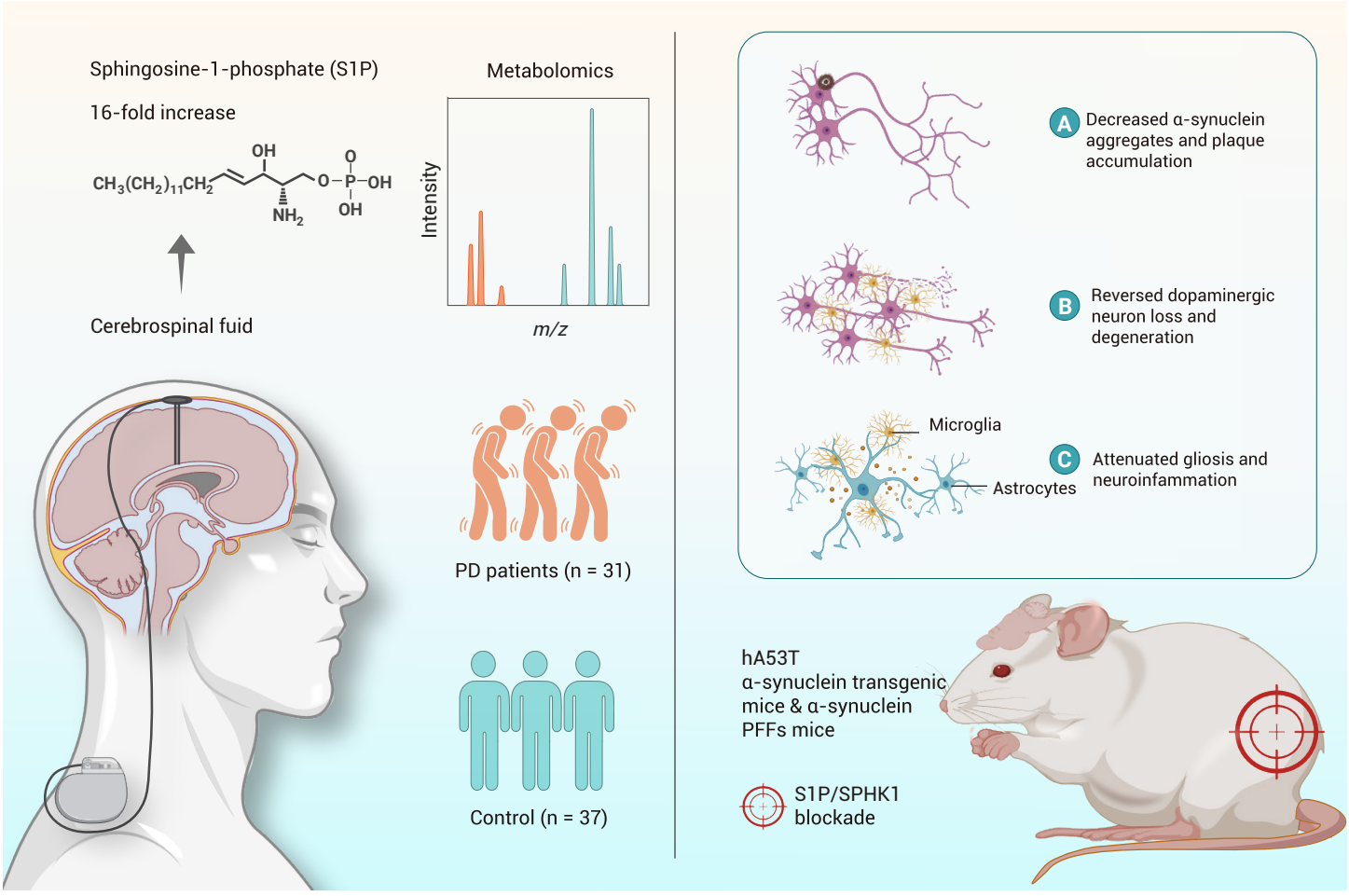

PUBLIC SUMMARY

- Sphingosine-1-phosphate is significantly elevated in the cerebrospinal fluid of Parkinson's disease patients.
- Pathologic α-synuclein selectively upregulates microglial SPHK1 over SPHK2.
- S1P-mediated NF-κB signaling triggers pathologic α-synuclein-induced microglial activation.
- Blockade of SPHK1 attenuates α-synuclein aggregation and neuroinflammation.

ARTICLE

OPEN ACCESS

www.the-innovation.org/life

Discovery of S1P/SPHK1 dysregulation in Parkinson's disease and its role in pathological α-synuclein-induced neurodegeneration

Jiacheng Fang,[1,8] Xiaoxiao Wang,[1,8] Xiuli Su,[2] Dan Li,[1] Fuyue Wang,[1] Pengxi Wang,[3] Chenrui Yuan,[1] Fenfen Ji,[1] Doudou Zhang,[4] Xiaodong Cai,[4] Wenlan Liu,[5] Min Li,[6] Shen Hu,[7] and Zongwei Cai[1,2,*]

[1]State Key Laboratory of Environmental and Biological Analysis, Department of Chemistry, Hong Kong Baptist University, Hong Kong SAR 999077, China
[2]Eastern Institute of Technology, School of Chemistry, Ningbo 315200, China
[3]Department of Biology, Hong Kong Baptist University, Hong Kong SAR 999077, China
[4]Department of Neurosurgery, The First Affiliated Hospital of Shenzhen University, Shenzhen Second People's Hospital, Shenzhen 518037, China
[5]The Central Laboratory, The First Affiliated Hospital of Shenzhen University, Shenzhen Second People's Hospital, Shenzhen 518037, China
[6]Mr. and Mrs. Ko Chi Ming Centre for Parkinson's Disease Research, School of Chinese Medicine, Hong Kong Baptist University, Hong Kong SAR 999077, China
[7]Jonsson Comprehensive Cancer Center, California NanoSystems Institute, School of Dentistry, University of California, Los Angeles 90024, USA
[8]These authors contributed equally
*Correspondence: zwcai@hkbu.edu.hk

Received: April 9, 2025; Accepted: October 13, 2025; Published Online: October 16, 2025; https://doi.org/10.59717/j.xinn-life.2025.100164

Citation: Fang J., Wang X., Su X., et al. (2025). Discovery of S1P/SPHK1 dysregulation in Parkinson's disease and its role in pathological α-synuclein-induced neurodegeneration. *The Innovation Life* **3**:100164.

Parkinson's disease (PD) manifests a significant lipidopathy, marked by an enrichment of risk genes involved in sphingolipid metabolism. Sphingolipids are master regulators of cell fate, with sphingosine-1-phosphate (S1P) acting as a key signaling mediator in immunology and vascular biology. However, the fluctuation of S1P metabolism in PD and its role in synucleinopathy-induced neurodegeneration remain poorly understood. In this study, we discovered a 16-fold increase in cerebrospinal fluid (CSF) S1P levels synthesized by sphingosine kinase 1 (SPHK1) in PD patients compared to controls, accompanied by a reduction in sphingosine levels. Similarly, elevated S1P levels are observed in the striatum and midbrain of the α-synuclein preformed fibrils (α-syn PFFs)-induced mouse model of sporadic PD, with *Sphk1* exhibiting the most pronounced upregulation among genes categorized under the "sphingosine metabolic process", while *Sphk2* expression remains unchanged. The increase of S1P levels is associated with the selective modulation of SPHK1 in microglia responding to pathological α-synuclein. Of note, α-syn PFFs treatment increases *Sphk1* expression and activates SPHK1 in microglia. SPHK1 serves as a key contributor to pathologic α-syn-induced microglial activation via S1P-mediated NF-κB signaling. Knockdown of microglial *Sphk1* alleviated neurodegenerative pathology in α-syn PFFs mice alleviates their neuropathological changes. Similarly, inhibition of SPHK1 with PF543 ameliorates PD-like neuropathological abnormalities in hA53T α-synuclein transgenic mice. These findings support a key role of S1P in the pathogenesis of PD linked to pathological α-synuclein.

INTRODUCTION

Parkinson's disease (PD) is the most common form of synucleinopathy and ranks as the fastest growing neurodegenerative disorder worldwide.[1,2] Its hallmark pathology includes the progressive degeneration of dopaminergic neurons in the substantia nigra pars compacta (SNpc) with a concurrent decrease in striatal dopamine secretion, alongside the neuronal buildup of Lewy bodies and Lewy neurites.[3] Despite symptomatic treatments being available, no current interventions efficiently slow down or halt disease progression.[1] To address this issue, advancing our understanding of PD pathogenesis and identifying innovative therapeutic targets is imperative.

Microglia play a broad role of in the pathogenesis of neurodegenerative diseases.[4–6] Genes enriched in microglia overlap significantly with those showing altered expression in neurodegenerative conditions.[7] Genetic variants linked to neurodegenerative disorders exhibit microglia-specific patterns of enhancer enrichment.[8] Upon exposure to injurious stimuli, microglia lose their essential housekeeping function[5] and drive neuroinflammation by releasing proinflammatory factors.[9] Specifically, activated microglia secrete IL-1α, TNF-α, and C1q, which induce astrocytes to become neurotoxic, a common feature in neurodegenerative and neuroinflammatory disorders.[10] Moreover, microglia in PD brain lesions harbor pathological α-synuclein inclusions, highlighting their role in disease progression.[11,12] This may be explained by the fact that neurons release monomeric and oligomeric α-synuclein via unconventional exocytosis,[13] while microglia actively internalize extracellular α-synuclein aggregates through a repertoire of highly expressed receptors (e.g., TREM2, CD36, LAG3, RAGE).[14–19] However, despite their rapid uptake of α-synuclein fibrils, microglia degrade them inefficiently, leading to their accumulation and triggering inflammatory responses that may contribute to neurodegeneration in PD.[20]

Sphingolipid metabolism imbalance links neurodegeneration.[21] Gaucher disease, the most common sphingolipid lysosomal storage disorder, is associated with an increased risk of early-onset parkinsonian symptoms.[22] The enrichment of PD-associated risk genes related to sphingolipid metabolism further highlights its dynamic regulation in disease states.[23] Among sphingolipid metabolites, ceramide and sphingosine-1-phosphate (S1P) play pivotal roles as signaling molecules in immunity and chronic inflammation.[24,25] Lactosylceramide (LacCer), a ceramide derivative, has been implicated in promoting chronic central nervous system (CNS) inflammation by modulating astrocytic pathogenic activity.[26,27] S1P is essential for angiogenesis[28] and neurogenesis[29], underscoring its broader significance in CNS health. However, excessive S1P disrupts the architecture and function of synapses[30] and axons[31], while reduced serum S1P levels in PD patients correlate with increased motor severity and faster disease progression.[32] In addition, S1P has been shown to activate the PI3K/Akt signaling pathway and confer anti-apoptotic protection in endothelial cells and to enhance Akt and nitric oxide production through Gi protein–mediated activation in endothelial models.[33,34] However, excessive PI3K/Akt–mTOR activation may suppress autophagy and thereby impair the clearance of α-synuclein aggregates.[35] GLP1R agonists, which have shown neuroprotective effects in both experimental models and clinical studies, also activate PI3K/AKT pathway.[36]

At present, it remains unclear whether S1P metabolism is dysregulated in the CSF of PD patients and whether such dysregulation contributes to synucleinopathy-driven neurodegeneration. Our study reveals significantly elevated levels of S1P in the CSF from PD patients, driven by pathologic α-synuclein accumulation. This elevation correlates with the differential regulation of sphingosine kinases in the microglial response to pathologic α-synuclein, where S1P plays a critical role in α-syn PFFs-induced microglial activation and the formation of pathologic α-synuclein aggregates. Our findings underscore S1P as a critical contributor to the pathogenesis of PD linked to pathologic α-synuclein, providing the possibility of investigating SPHK1 as a potential target for PD and other synucleinopathy-driven neurodegenerative disorders.

MATERIALS AND METHODS

Animals

Three-month-old male C57BL/6 mice used for stereotaxic injection of α-syn PFFs were obtained from the Laboratory Animal Service Centre at The Chinese University of Hong Kong. Male hA53T α-syn transgenic mice were sourced from Jackson Laboratories (C57BL/6; Prnp-SNCA×A53T). All experi-

mental procedures complied with guidelines from Hong Kong Baptist University (HKBU) for the use of experimental animals and were approved by the HKBU Committee on the Use of Human & Animal Subjects in Teaching and Research.

α-syn PFFs preparation

Mouse α-synuclein monomers (RP-009, PROTEOS) with endotoxin levels below 0.0583 EU/mg were used to generate preformed fibrils. Monomers in TBS (10 mM Tris, 50 mM NaCl, pH 7.6) were diluted in an equal volume of 2× PBS (pH 7.4-7.6) to a final concentration of 5 mg/mL, providing appropriate ionic strength for fibril formation. This solution was incubated in a ThermoMixer at 37°C with shaking at 900 rpm for 5 days. The resulting aggregates were diluted to 0.1 mg/mL with PBS and sonicated on ice at 20% amplitude for 180 s (0.5s on/0.5s off).

Stereotaxic injection of α-syn PFFs

Three-month-old C57BL/6 mice were anesthetized with isoflurane in oxygen and positioned in a stereotaxic alignment system with the following coordinates: 2.0 mm (mediolateral) relative to Bregma, 0.2 mm (anteroposterior), 2.6 mm (dorsoventral). The infusion was performed at a rate of 0.2 μl per min, and a total of 2.5 μl of α-syn PFFs (2.0 μg/μl in PBS) or vehicle was unilaterally injected into the striatum of the right hemisphere using a 10-μl Hamilton syringe (701 N, Hamilton) fitted with a cemented 26.5-gauge needle. After infusion, the needle was held in place for 5 min before being slowly withdrawn.

Molecular cloning

To create a catalytically inactive SPHK1 (D81A), the Q5 Site-Directed Mutagenesis Kit (E0554S, NEB) was used to replace the 81st Asp residue with Ala in the HsSPHK1 plasmid (118091, addgene). The resulting plasmid served as a template to amplify the mutated SPHK1 coding sequence, which was then cloned into the BamHI-XhoI sites of the pcDNA3.1 vector.

To construct the *Sphk1*-targeting and non-targeting shRNA vectors, a 328 bp DNA fragment was synthesized. This fragment contained the mir30-shRNA backbone with either the *Sphk1* shRNA sequence (5′-CCTACTCTGTCTAGGCTGAGAT-3′) or a control shRNA sequence (5′-CAGGAATTATAATGCTTATCTA-3′). The mir30-shRNA cassette was then cloned into the pLenti-CD11b plasmid between the PstI and NotI restriction sites.

Electroporation transfection

BV2 microglial cells were trypsinized to obtain 1.5×10^7 cells, washed with Ca^{2+}/Mg^{2+}-free PBS, and resuspended in Resuspension Buffer R (N10025, Thermo Scientific) at a density of 3.0×10^7 cells/mL. Electroporation transfection was performed using Neon NxT Electroporation System (NEON1S, Thermo Scientific) with 100-μL Neon NxT tips (N10025, Thermo Scientific). For each electroporation, 10 μg of plasmid DNA was mixed with 100 μL of the cell suspension, loaded into a Neon NxT tip, and placed in a Neon Tube positioned within Neon Pipette Station. The electroporation parameters were set as follows: 900 V pulse voltage, 20 ms pulse width, and 2 pulses. After electroporation, the cells were cultured in prewarmed serum-containing medium without antibiotics.

Lentivirus packaging

Lentivirus particles were produced by transfecting 293T cells at about 90% confluence in T175 flasks with 30 μg of either pLenti-CD11b-mir30-shRNA vector or pGreenFire NF-κB Reporter Lentivector (TR412PA-P, System Biosciences), together with 18 μg of pGP and 12 μg of pVSVG_pMD2.G. The culture medium was changed at 6 and 24 h post-transfection. Cells were maintained for an additional 48 h, after which the viral supernatant was collected, filtered through 0.45 μm PVDF filters, and mixed with Lenti-X concentrator (631231, Clontech) at a 3:1 ratio. The mixture was centrifuged at 1,500 g for 45 min at 4°C to pellet lentivirus particles. Viral titers were measured using Lenti-X qRT-PCR Titration Kit (631235, TaKaRa) following the manufacturer's instructions.

Statistical analysis

Statistical analyses were performed using Prism 9 software (GraphPad), typically employing an unpaired t-test or a two-way ANOVA, both with parametric settings. Post-hoc pairwise comparisons were conducted following ANOVA using the Tukey correction to adjust for multiple comparisons. For the human data, analysis of covariance (ANCOVA) was performed to adjust for age and sex when comparing metabolite levels among groups. The experimental mice were categorized based on their weight, and then randomly selected for grouping. All data were presented as mean ± standard deviation from a minimum of three biological replicates. Outliers were identified using ROUT method with a Q coefficient of 1% and were excluded from statistical analysis. Specific details on statistical tests and sample sizes are provided in the figures and their respective legends. Levels of probabilities less than 0.05 were considered statistically significant.

RESULTS

Metabolomic profiling and S1P dysregulation in synucleinopathy-induced PD

To investigate metabolomic alterations in PD, we performed a global metabolic profiling of the CSF samples from a well-characterized cohorts comprising 68 subjects. The demographic characteristics of participants showed no significant differences in age or sex distribution between PD patients and control subjects (Table 1). Using liquid chromatography-tandem mass spectrometry (LC-MS/MS), we identified significant metabolic disruptions in PD patients. The analysis with high-resolution mass spectrometry detected 3,219 features in the positive ionization mode and 2,932 features in the negative ionization mode in the CSF samples from PD patients, of which 1,462 and 1,343 features, respectively, showed significant differences between PD patients and controls. Partial least squares discriminant analysis (PLS-DA) based on two principal components effectively distinguished the control and PD groups (Figures S1A-B), as evidenced by high R2Y values (0.983 and 0.986 for positive and negative ionization mode, respectively) and Q2 values (0.891 and 0.907 for positive and negative ionization mode, respectively) that indicated good predictive accuracy. A permutation test (n = 999) confirmed the absence of overfitting (Figures S1C-D). Notably, S1P was the most significantly elevated metabolite (Figures 1A-B & Table S1), with its relative abundance in the CSF from PD patients being 16 times higher than in controls. Meanwhile, the levels of its precursor, sphingosine, were significantly reduced (Figure 1C), indicating that enhanced SPHK1 activity driving accelerated conversion of sphingosine to S1P. Supporting this, S1P and sphingosine levels were positively correlated in the control group, but this correlation was abolished in the context of PD (Figure 1D). As previously demonstrated,[37] plasma S1P levels were significantly lower in PD patients than in controls, accompanied by a substantial reduction in plasma sphingosine. These results collectively suggested the metabolic compartmentalization of S1P and sphingosine in PD. We then characterized changes in S1P levels in the CSF during aging. In healthy controls, CSF S1P levels gradually declined with age (Figure 1D). However, this age-related reduction was absent in PD patients (Figure 1D), indicating a disruption of S1P metabolic regulation associated with PD. To explore the clinical relevance of this dysregulation, we examined the relationship between CSF S1P levels and behavioral deficits. A significant correlation was observed between elevated S1P levels and the severity of behavioral deficits in PD patients (Figure 1D), whereas no such correlation was found for sphingosine levels, underscoring the potential role of S1P dysregulation in PD pathology. Additionally, the discriminative ability of S1P was assessed through receiver operating characteristic (ROC) curve analysis, yielding the areas under the curve (AUC) of 0.95 for CSF (Figure 1E).

Given the central role of α-synuclein misfolding and aggregation in PD development, we investigated whether α-synuclein fibrils could induce S1P production *in vivo*. To address this, we used a sporadic PD model with the intrastriatal injection of α-syn PFFs (Figures S2A-C) in mice and examined the S1P abundance in the dissected brains of the model animals. S1P was predominantly localized to the striatum and midbrain (Figure S1E), the areas strongly implicated in PD pathogenesis.[1,2] This is further supported by the spatial distribution of *Sphk1* predominantly in the ventral midbrain of mice (Figure S1F). In contrast, *Sphk2* exhibited non-region-specific expression across the brain. Similar to the cohort study, elevated levels of S1P were also detected in the striata and midbrains of model mice (Figure 1F). In addition,

Table 1. The demographic characteristics of the recruited participants.

Characteristics	Gender (Males/females)	Age (Years)	H-Y stage [a]	N
PD	18/13	59.48 ± 7.54	2.74 ± 0.69	31
Control	23/14	55.31 ± 12.20	–	37
P-value [b]	0.12	0.14	–	–

[a] Severity of disease and H-Y stage values are expressed as mean ± s.d. [b] The chi-square test was used to compare gender distribution, and the t-test was applied to assess age differences.

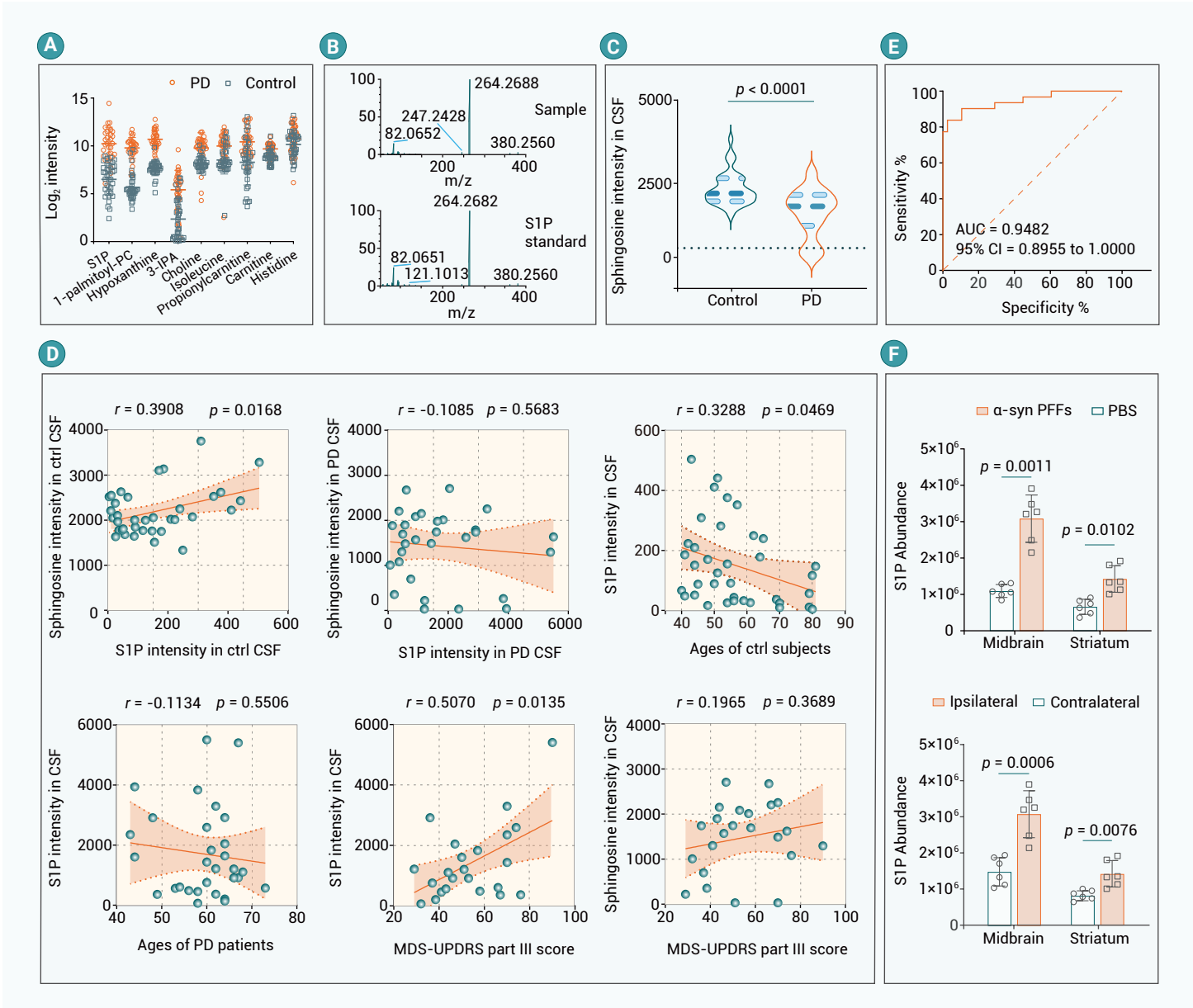

Figure 1. Metabolomic profiling and S1P dysregulation in synucleinopathy-induced PD (A) Intensity of elevated metabolites in the CSF of PD patients (n = 31) compared to that in control subjects (n = 37). (B) The MS^2 spectrum of S1P in sample and S1P standard. (C) Quantification of sphingosine in the CSF from PD patients (n = 31) and control individuals (n = 37), unpaired t test. (D) Correlation analyses of CSF S1P intensity with sphingosine intensity, age, and MDS-UPDRS part III score in control individuals and PD patients. (E) ROC analysis for S1P in the CSF of PD patients (n = 31), Wilson/Brown method. (F) S1P abundance in the midbrains and striata of mice stereotaxically injected with either α-syn PFFs or vehicle (n = 6, mean ± s.d, unpaired t test).

S1P levels were found to be significantly higher in the striatum and midbrain ipsilateral to the injection site of α-syn PFFs compared to the contralateral side (Figure 1F). These findings suggest the pathological elevation of S1P levels in the context of synucleinopathy-induced PD.

Selective upregulation of microglial SPHK1 in response to pathological α-synuclein

S1P is a key signaling lipid produced by SPHK1 and SPHK2 in the biosynthetic pathway of sphingolipids (Figure 2A). To explore the changes in the expression of genes categorized under the "sphingosine metabolic process" in Gene Ontology, we used a transgenic PD model with progressive neurodegeneration, which constitutively expresses the human α-synuclein gene with A53T (hA53T) mutation.[38] We found that the gene expression of SPHK1 was selectively upregulated relative to SPHK2 in the brains of hA53T mice compared with age-matched wild-type (WT) littermates (Figure 2B). Congruently, in post-mortem brain lesions from PD patients, *SPHK1* expression was

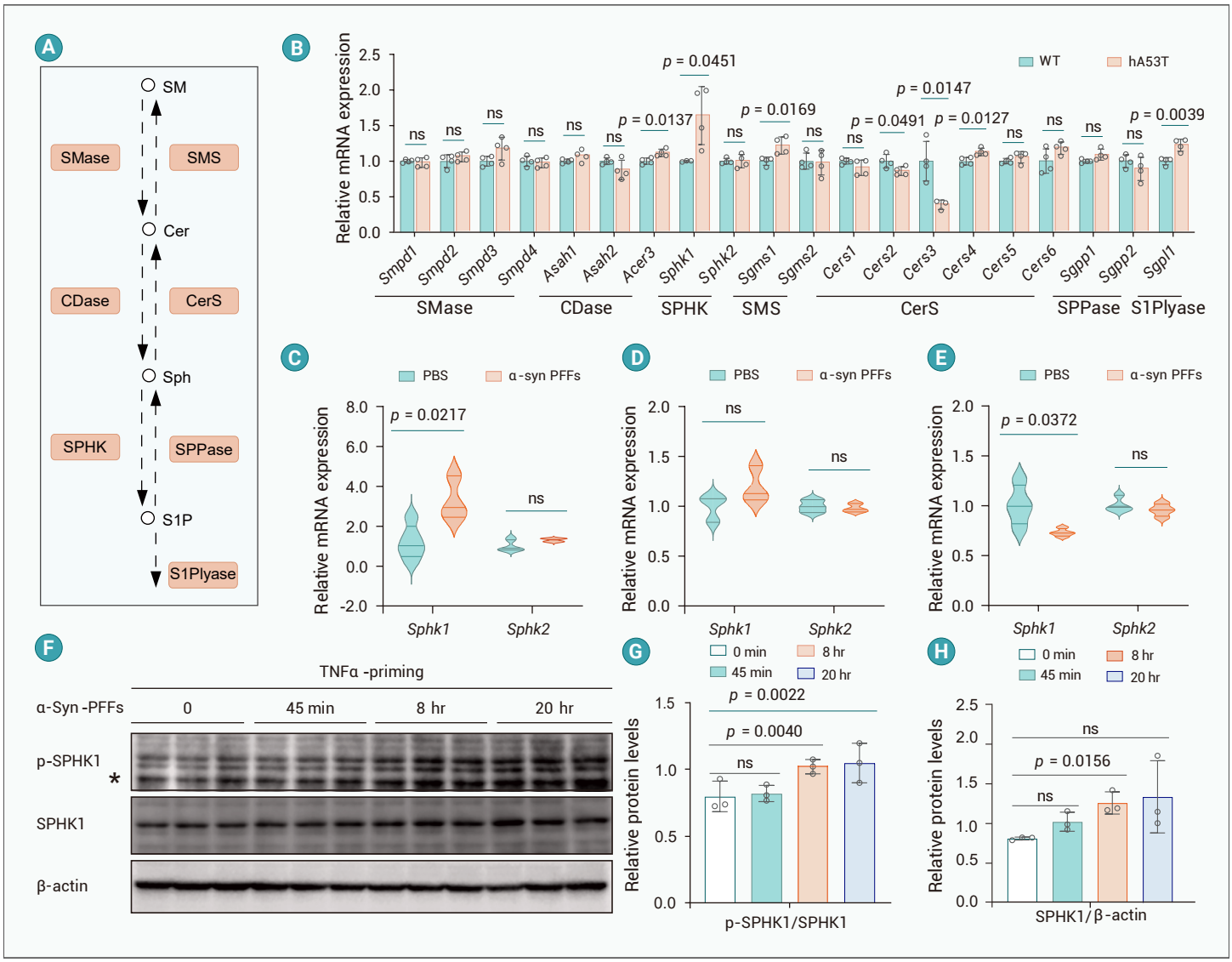

Figure 2. Selective upregulation of microglial SPHK1 in response to pathological α-synuclein (A) Biosynthetic pathway of sphingolipids. (B) Relative mRNA expression of sphingolipid metabolism-related genes in the brainstem of hA53T α-syn transgenic mice compared to WT mice (n = 4, mean ± s.d, unpaired t test). (C) Relative expression of *Sphk1* and *Sphk2* in mouse primary microglia treated with α-syn PFFs compared to control (n = 3-6, unpaired t test). (D) Relative expression of *Sphk1* and *Sphk2* in mouse primary astrocytes treated with α-syn PFFs compared to control (n = 3, unpaired t test). (E) Relative expression of *Sphk1* and *Sphk2* in mouse primary neurons treated with α-syn PFFs compared to control (n = 4, unpaired t test). (F) SPHK1 phosphorylation (Ser225, p-SPHK1) in microglia treated with α-syn PFFs (n = 3), the asterisk indicates non-specific band. (G) Quantification of the levels of p-SPHK1 in microglia normalized to SPHK1 (n = 3, mean ± s.d, two-way ANOVA). (H) Quantification of the levels of SPHK1 in microglia normalized to β-actin (n = 3, mean ± s.d, two-way ANOVA).

significantly increased in the substantia nigra, whereas *SPHK2* exhibited no discernible change (Figure S3). In contrast, the expression of *Cers2* and *Cers3* were significantly downregulated in the brains of hA53T mice compared with controls (Figure 2B). Given that sphingosine can be re-converted into ceramide by ceramide synthase (CerS) (Figure 2A), the decreased expression of *Cers2* and *Cers3* suggested that the sphingosine salvage pathway was probably not excessively activated.

Strong evidence suggests that glia convert very-long-chain fatty acids into S1P through a glial-specific pathway,[39] and mammalian *SPHK1* homologs exhibit highly enriched expression in specific glial subpopulations.[40,41] Based on this, we further explored whether microglia were the predominant cell type that upregulates *Sphk1* expression in response to α-syn PFFs. α-syn PFFs treatment led to a significant increase of *Sphk1* expression in microglia, while having no effect on its expression in astrocytes and decreasing its expression in neurons (Figures 2C-E). In contrast, *Sphk2* expression remained unchanged in both glial cells and neurons following α-syn PFFs exposure (Figures 2C-E). To investigate the impact of α-syn PFFs on microglial SPHK1 activity, we evaluated the level of SPHK1 phosphorylation (Ser225, p-SPHK1) in microglia treated with α-syn PFFs. Prolonged exposure to α-syn PFFs was observed to significantly increase p-SPHK1 levels in microglia (Figures 2F-H). Taken together, the findings suggest that microglial SPHK1, rather than SPHK2, undergoes upregulation in response to pathological α-synuclein.

S1P mediates α-syn PFFs-induced microglia activation

Given that S1P acts as a cofactor for TNF receptor-associated factor 2 essential for its E3 ligase activity,[42] we examined the gene expression correlations between *SPHK1* and NF-κB target genes using the data from the Genotype Tissue Expression (GTEx) database. *SPHK1* expression showed a strong positive correlation with *TNF*, *IL1A*, and *IL6* expression in the putamen, caudate, and substantia nigra regions of human brain, whereas *SPHK2* expression was weakly correlated (Figures 3A-B & Figure S4). This suggests a potential association between *SPHK1* and neuroinflammation. Likewise, in other normal human organs, *SPHK1* shows a stronger correlation with inflammation than *SPHK2* (Figure S5). In hA53T mice, there was an upregulation of hallmark genes related to the inflammatory response, which was attenuated in the mice treated with PF543 (Figure 3C). To ascertain the involvement of SPHK1 versus SPHK2 in α-syn PFFs-induced inflammation, we measured the transactivation activity of NF-κB in microglia treated with α-syn PFFs and PF543, a selective SPHK1 inhibitor, or ABC294640, a selective SPHK2 inhibitor (Table S2). PF543 pretreatment abolished the increase in NF-κB

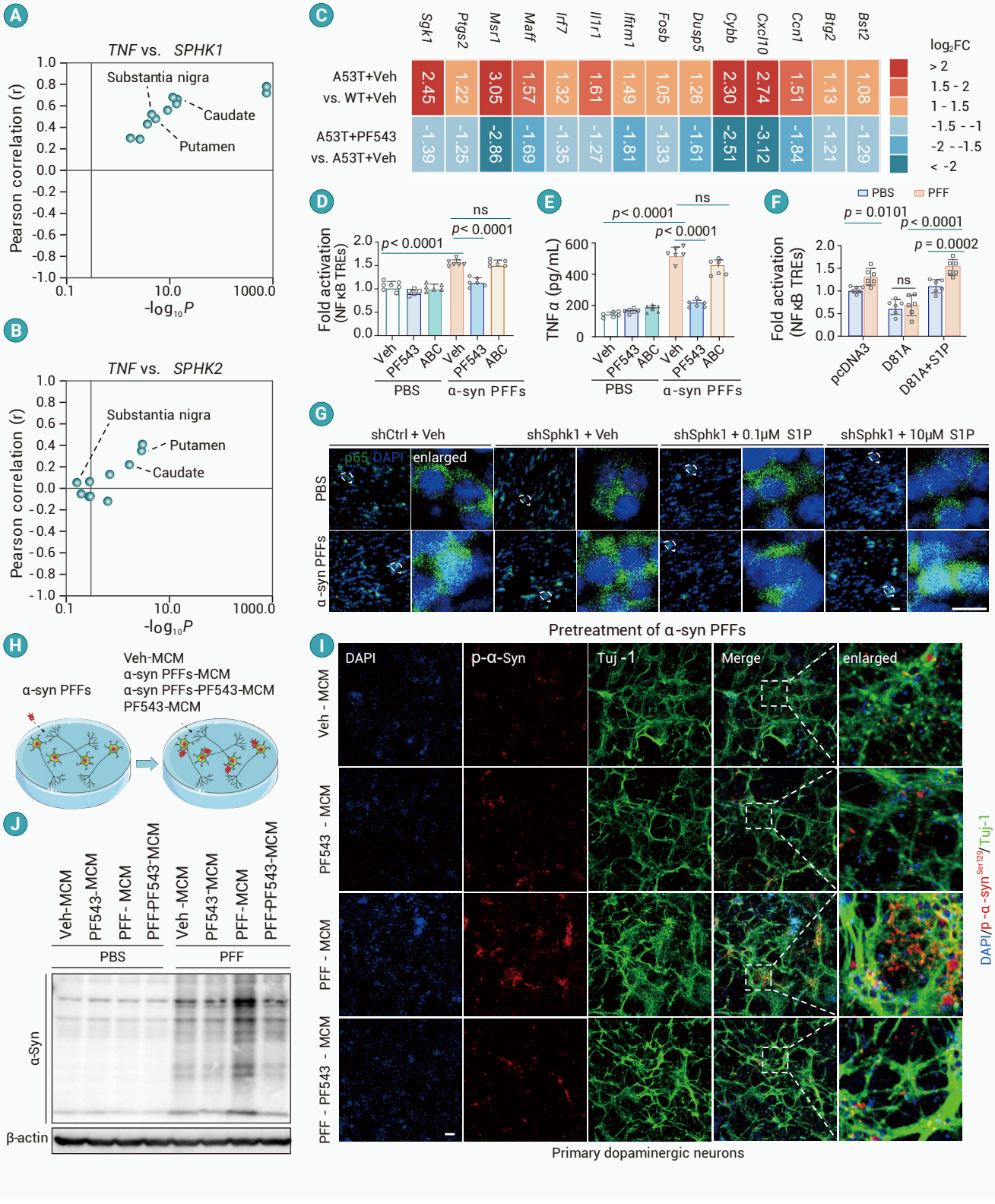

Figure 3. Blockade of microglial SPHK1 alleviates pathological α-synuclein formation by suppressing S1P-mediated NF-κB activation (A) Correlation of *SPHK1* expression with *TNF* expression in various brain regions based on the data from GTEx database. (B) Correlation of *SPHK2* expression with *TNF* expression in various brain regions based on the data from GTEx database. (C) Differential expression of representative hallmark genes associated with inflammation response and TNFα signaling via NF-κB (n = 4, Wald test). (D) Reporter gene activity of NF-κB-responsive luciferase in BV2 microglia induced by α-syn PFFs following exposure to either PF543 or ABC294640 (n = 6, mean ± s.d, two-way ANOVA). (E) TNFα levels in mouse primary microglia induced by α-syn PFFs following exposure to either PF543 or ABC294640 (n = 6, mean ± s.d, two-way ANOVA). (F) α-syn PFFs-induced reporter gene activity of NF-κB responsive luciferase in BV2 microglia following transfection with SPHK1 Asp81Ala mutant and exposure to either S1P supplementation or vehicle (n = 6, mean ± s.d, two-way ANOVA). (G) The DNA binding of p65 induced by α-syn PFFs in BV2 microglia was abolished upon the knockdown of *SPHK1*, and this effect was reversed by 10 μM S1P supplementation. Scale bar, 20 μm (original) and 10 μm (enlarged). (H) Schematic diagram showing treatment of MCM into primary dopaminergic neurons, which were pretreated with PBS or α-syn PFFs for 1 day. (I) Representative double-immunostaining for p-α-syn^{ser129} (red) and Tuj-1 (green) in primary dopaminergic neurons (n = 3). Scale bar, 25 μm. (J) Representative immunoblots of α-synuclein and β-actin in the Triton X-100-insoluble fractions.

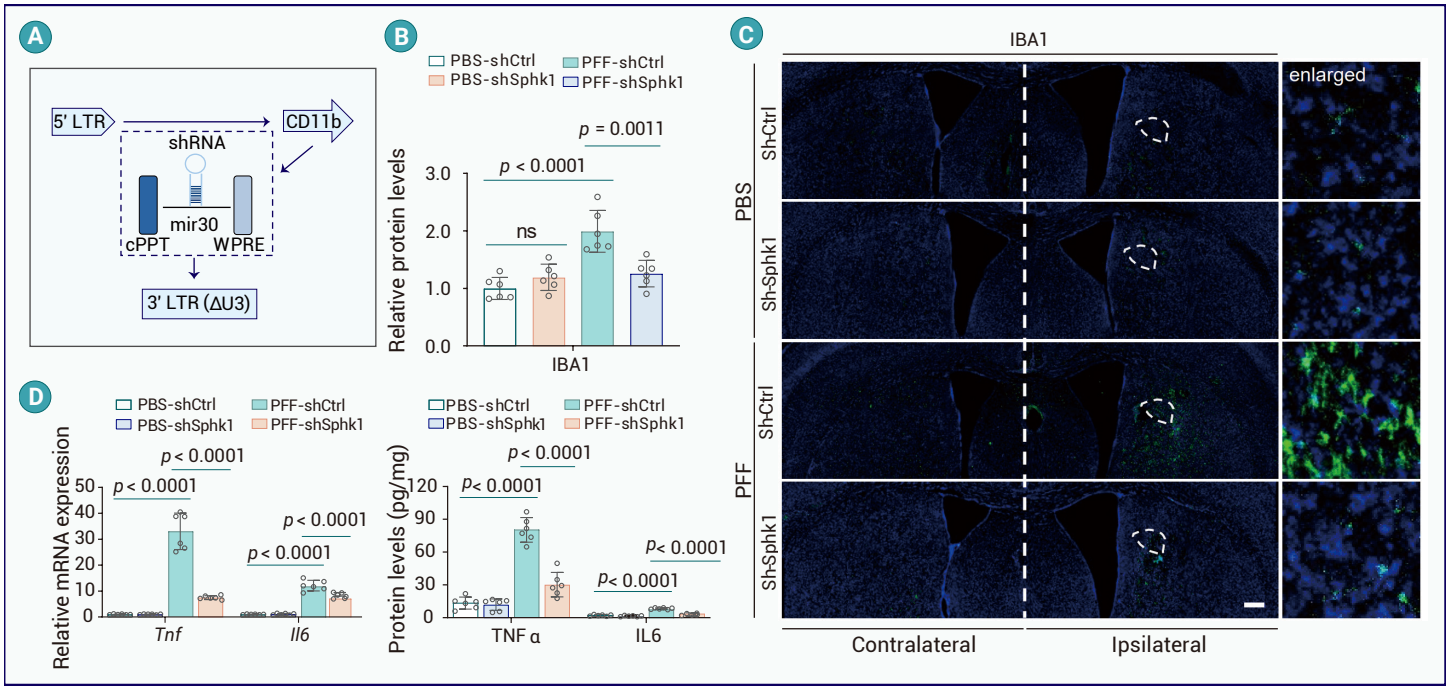

Figure 4. ***Sphk1*** **knockdown alleviates α-syn PFFs-induced neuroinflammation** (A) Scheme of the microglia-specific mir30-shRNA lentivector. (B) Quantification of IBA1 levels in the striata normalized to β-actin (n = 6, mean ± s.d, two-way ANOVA). (C) Immunofluorescence of IBA1 (green) in the striatum ipsilateral and contralateral to the injection site of α-syn PFFs and mir30-shRNA lentivirus. Scale bar, 200 μm. (D) The relative mRNA expression levels of *Tnf* and *Il6* in the motor cortices of mice (n = 6, mean ± s.d, two-way ANOVA). The protein levels of TNFα and IL6 in the motor cortices of mice (n = 6, mean ± s.d, two-way ANOVA).

transactivation activity induced by α-syn PFFs, as evidenced by a reduced NF-κB responsive luciferase reporter gene signal (Figure 3D). Consistently, PF543 suppressed the α-syn PFFs-induced elevation in TNFα levels (Figure 3E). In contrast, ABC294640 failed to reduce the increased NF-κB transactivation activity and the elevated TNFα levels in microglia following α-syn PFFs treatment (Figures 3D-E). These findings indicate that microglial SPHK1 plays a vital role in fibrillar α-synuclein-induced microglia activation.

To investigate the dependence of α-syn PFFs-induced microglial activation on S1P, we examined inflammation in BV2 microglia transfected with a loss-of-function mutation of SPHK1 (Asp81Ala, D81A), which lacks activity for phosphoryl transfer and adenosine diphosphate formation.[43] Overexpression of SPHK1 (D81A) suppressed signals from the α-syn PFFs-induced NF-κB responsive luciferase reporter gene, which was reversed by supplementation with 10 μM S1P (Figure 3F). Additionally, SPHK1 (D81A) overexpression inhibited the elevated levels of TNFα induced by α-syn PFFs, and this inhibition was also reversed by S1P supplementation (Figure S6). Moreover, exposure of BV2 microglia to α-syn PFFs resulted in significant nuclear translocation of p65, a hallmark of NF-κB activation (Figure 3G). Besides, knockdown of *Sphk1* using mir30 shRNA resulted in substantial cytoplasmic retention of p65, which was reversed by supplementation with 10 μM S1P (Figure 3G). However, we did not observe translocation of p65 to the nuclei in *Sphk1*-silenced BV2 microglia treated with 100 nM exogenous S1P, a concentration that exceeds the dissociation constant values for all S1P receptors but does not increase intracellular S1P levels (Figure 3G). This indicates that S1P does not activate NF-κB through a paracrine manner acting on cell surface receptors. Together, our findings illustrate that α-syn PFFs-induced microglial activation critically depended on intracellular S1P.

Inhibition of microglial SPHK1 alleviates pathological α-synuclein formation

To investigate the involvement of SPHK1 in PD pathogenesis through microglial action, we collected microglial-conditioned medium (MCM) from α-syn PFFs-treated microglia, which were pretreated with PF543 or vehicle, and applied it to mouse primary dopaminergic neurons in the presence or absence of α-syn PFFs (Figure 3H). PF543 attenuated the α-syn PFFs-induced increase in NF-κB target protein levels in microglia (Figures S7A-B), indicating a reduction in inflammatory response. Notably, it was observed that pretreatment of microglia with PF543 significantly reduced the levels of p-α-syn^{Ser129} in neurons, which were induced by α-syn PFFs-treated MCM (Figures 3I & S7C). Congruently, the amount of pathologic Triton X-100-insoluble α-synuclein in primary dopaminergic neurons was reduced (Figure 3J). In contrast, direct pretreatment of neurons with PF543 failed to reduce the levels of p-α-syn^{Ser129} induced by α-syn PFFs-treated MCM (Figure S8). These results indicate that inhibiting the kinase activity of microglial SPHK1 could mitigate the formation of pathological α-synuclein in neurons induced by α-syn PFFs.

Microglia-specific knockdown of *Sphk1* diminishes α-syn PFFs-induced neuropathology

To investigate the therapeutic potential of targeting microglial *Sphk1* in PD *in vivo*, we knocked down *Sphk1* expression in striatal microglia using lentivirus-delivered short-hairpin RNA (shRNA) expression driven by the *Itgam* (CD11b-encoding) promoter (Figures 4A & S9A-B).[44] Western blot analysis revealed a reduction in pathologic Triton X-100-insoluble α-synuclein levels in the striata following *Sphk1* knockdown (Figure S9C). Besides, *Sphk1* knockdown attenuated the elevation of ionized calcium-binding adapter (IBA1) levels induced by α-syn PFFs in the striata and midbrains ipsilateral to the injection side (Figures 4B-C & S9D-F), suggesting suppressed microglial activation by *Sphk1* knockdown. *Sphk1* knockdown also suppressed the mRNA levels and protein levels of TNFα and IL6 in α-syn PFFs model mice (Figure 4D). The above results underscore that microglial SPHK1 plays a vital role in promoting α-syn PFFs-induced PD-like pathology in mouse models.

SPHK1 inhibition alleviates α-syn PFFs-induced PD-like neuropathology in mice

PF543, which has a 100-fold selectivity for SPHK1 over SPHK2 and sphingosine-competitive properties,[45] was chosen and evaluated for its ability to penetrate the blood-brain barrier. Our results showed that a single intraperitoneal injection of PF543 (10 mg/kg) in naïve mice resulted in an elimination half-life of 0.27 ± 0.02 h and reached therapeutically relevant concentrations in the plasma (Figure S10A & Table S3). Accordingly, plasma S1P levels progressively decreased following PF543 administration (Figure S10B). In the midbrain, PF543 demonstrated a relatively long elimination half-life of 0.80 ± 0.18 h, with its concentration peaking around 30 min (Figure S8C & Table S3). S1P levels were also significantly reduced in the midbrains of mice with

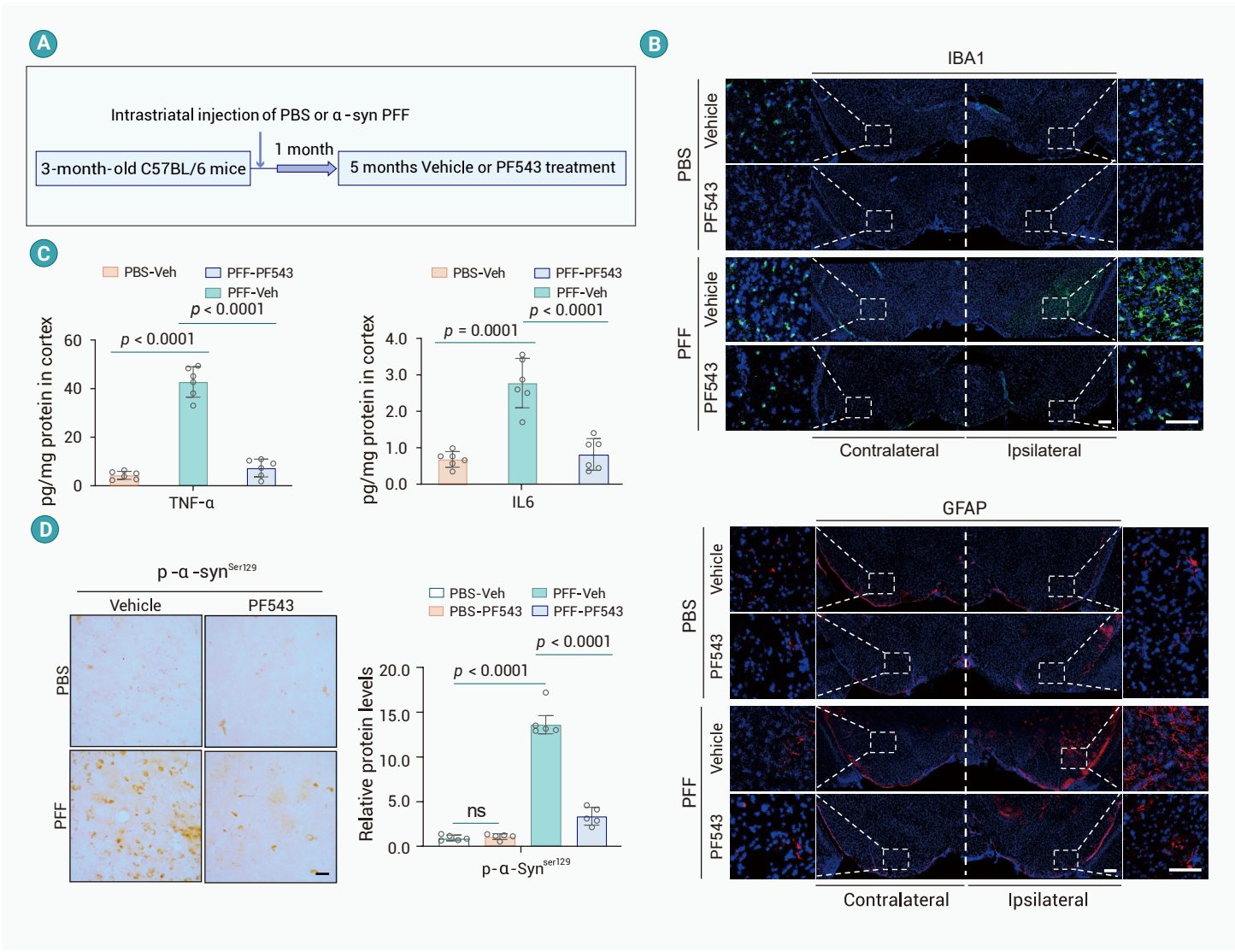

Figure 5. SPHK1 inhibition diminishes α-syn PFFs-induced PD-like neuropathology (A) Scheme of vehicle or PF543 treatment in mice stereotaxically injected with either α-syn PFFs or PBS. (B) Immunostaining of IBA1 (green) and GFAP (red) in the ventral midbrain. Scale bar, 200 μm (original) and 500 μm (enlarged). (C) TNFα and IL6 levels in the motor cortices of α-syn PFFs mice treated with either vehicle or PF543 (n = 6, mean ± s.d, two-way ANOVA). (D) Immunohistochemistry of p-α-syn^{ser129} in the striata. Scale bar, 20 μm. Quantification of p-α-syn^{Ser129} immunoreactivity intensity in the striata (n = 5, mean ± s.d, two-way ANOVA).

PF543 treatment (Figure S10D).

To ascertain whether SPHK1 inhibition can repress α-syn PFFs-induced microglial and astrocytic activation *in vivo*, mice were administered 10 mg/kg PF543 twice weekly for five months following the intrastriatal injection of α-syn PFFs (Figure 5A). As previously reported,[46] α-syn PFFs significantly increased IBA1 and glial fibrillary acidic protein (GFAP) immunoreactivity in the SNpc (Figure 5B). This increase was markedly reduced by PF543 treatment (Figure 5B). Western blot analysis further confirmed the increased levels of IBA1 and GFAP in the striata and ventral midbrains induced by α-syn PFFs and the reduction with SPHK1 inhibition (Figures S11A-D). Additionally, PF543 treatment markedly reduced the levels of neuroinflammatory factors TNFα and IL6 in the motor cortices of α-syn PFFs mice (Figure 5C). These results indicate that SPHK1 blockade effectively mitigate α-syn PFFs-induced neuroinflammation *in vivo*.

To investigate the neuroprotective potential of SPHK1 inhibition in the α-syn PFFs model, we administered PF543 one month after the intrastriatal injection of α-syn PFFs, a time point evidenced by hyperphosphorylated α-synuclein deposits.[47] Consistent with prior findings, substantial p-α-syn^{Ser129}-positive Lewy bodies were accumulated in the injection side of the striata (Figure 5D). PF543 significantly reduced p-α-syn^{Ser129} immunoreactivity in this area (Figure 5D). In addition, α-syn PFFs seeding induced a significant reduction in tyrosine hydroxylase (TH) and dopamine transporter (DAT) levels in the ventral midbrains, which was significantly rescued by PF543 (Figures S11E-F). Similarly, PF543 treatment restored TH and DAT levels in the striata ipsilateral to the injection of α-syn PFFs (Figures S11G-H).

SPHK1 inhibition reverses the neuropathology in hA53T α-synuclein transgenic mice

The effects of SPHK1 inhibition were further assessed in a transgenic mouse model of human *SNCA* harboring a PD-associated hA53T mutation. These mice manifest hyperactivity of pathological α-synuclein accumulation and reactive gliosis at four to six months old.[38] Accordingly, PF543 treatment in the hA53T transgenic mice was started at six months of age (Figure 6A). Consistent with previous results,[38] substantial p-α-syn^{Ser129}-positive inclusions were accumulated in the midbrain, cerebellum, and brainstem (Figures 6B-E). PF543 significantly reduced p-α-syn^{Ser129} immunoreactivity across these regions. Additionally, there was a significant decrease in the high-molecular-weight Triton X-100-insoluble α-synuclein levels (Figures 6F & S12A). PF543 treatment also attenuated reactive gliosis, another neuropathological hallmark. Specifically, Western blot analysis indicated abundant IBA1 and GFAP levels in the midbrains of hA53T mice but not in that of the mice treated with PF543 (Figures S12B-C). Immunostaining also revealed heightened GFAP immunoreactivity in hA53T mice, which was significantly mitigated by PF543 (Figure S12D). In healthy brains, microglia are typically ramified with small somas, but they undergo hypertrophic changes in response to stimuli[48]. Morphological analysis of microglia in

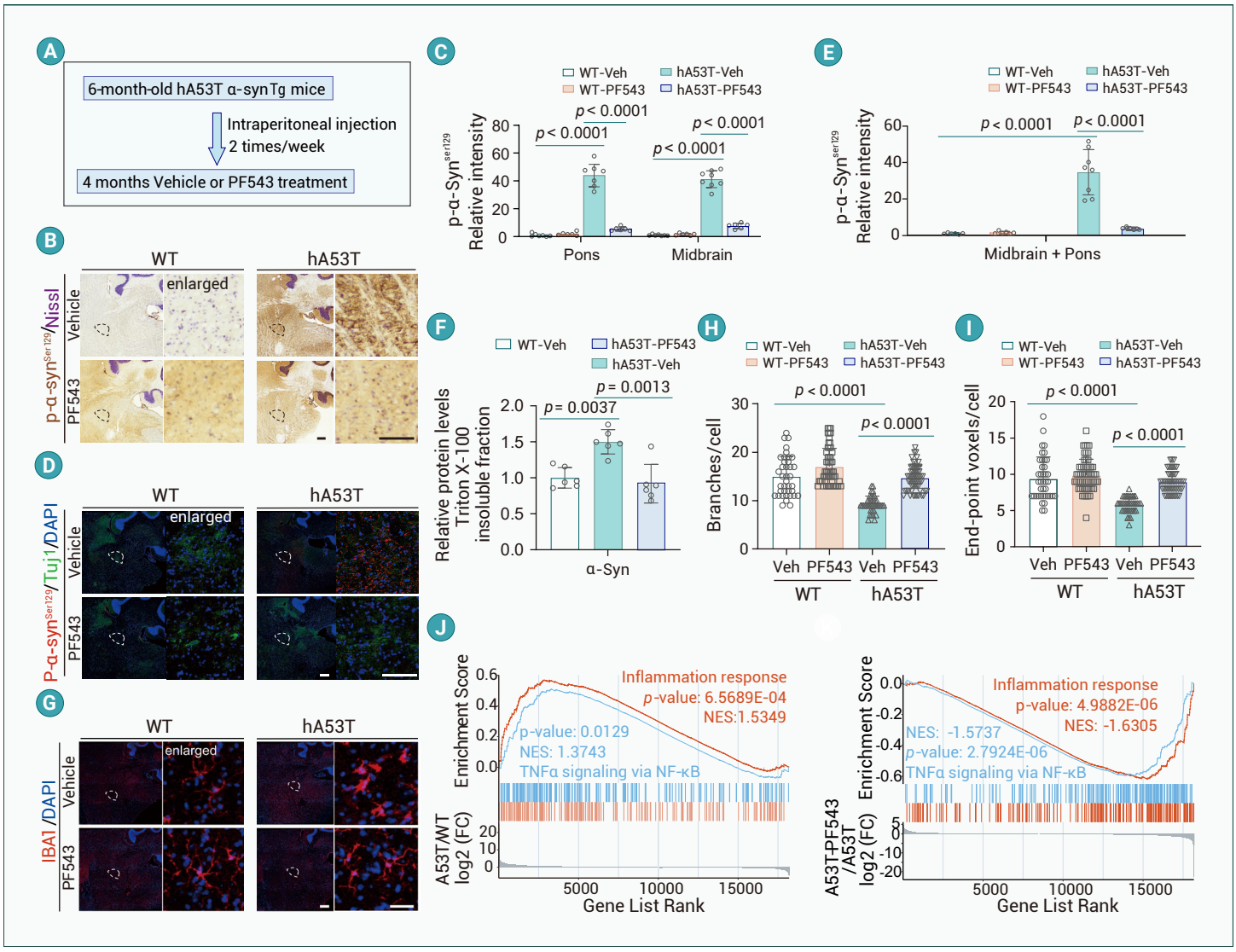

Figure 6. SPHK1 inhibition reverses the neuropathology in hA53T α-synuclein transgenic mice (A) Scheme of vehicle or PF543 treatment in hA53T α-synuclein transgenic mice. (B) Immunohistochemistry of p-α-syn^{Ser129} in the midbrain, pons, and cerebellum (n = 8). Scale bar, 250 μm. (C) Quantification of p-α-syn^{Ser129} immunohistochemistry intensity in the midbrain and pons (n = 8, mean ± s.d, two-way ANOVA). (D) Immunofluorescence of p-α-syn^{Ser129} in the midbrain, pons, and cerebellum (n = 8). Scale bar, 250 μm. (E) Quantification of p-α-syn^{Ser129} immunofluorescence intensity in the midbrain and pons (n = 8, mean ± s.d, two-way ANOVA). (F) Quantification of α-synuclein levels in Triton X-100 insoluble fractions normalized to β-actin (n = 6, mean ± s.d, two-way ANOVA). (G) The morphology of IBA1-staining microglia in the brainstems of WT and hA53T mice treated with either vehicle or PF543 (n = 6). Scale bar, 200 μm (original) and 20 μm (enlarged). (H) Number of dendrite segments of microglia in the brainstems of WT and hA53T mice treated with either vehicle or PF543 (mean ± s.d, two-way ANOVA). (I) Number of dendrite terminal points of microglia in the brainstems of WT and hA53T mice treated with either vehicle or PF543 (mean ± s.d, two-way ANOVA). (J) GSEA of RNA-sequencing data from hA53T and WT mice, as well as hA53T mice treated with either vehicle or PF543 (n = 4, Kolmogorov–Smirnov test).

hA53T mice indicated a reactive phenotype, with enlarged somas (Figure 6G) and a fewer number of branches and terminal points (Figures 6H-I). These abnormal alterations were significantly disappeared in hA53T mice treated with PF543 (Figures 6G-I). To further investigate the effects of SPHK1 inhibition on CNS transcriptional program, we conducted a transcriptome analysis of hA53T mice treated with either vehicle or PF543 using RNA sequencing. In hA53T mice, there was increased expression of hallmark genes associated with the inflammatory response and TNFα signaling via NF-κB, which was suppressed in the mice receiving PF543 (Figures 6J & S12E). These results demonstrate that SPHK1 inhibition confers protection against the degenerative effects of constitutive hA53T α-synuclein expression in transgenic mice.

DISCUSSION AND CONCLUSION

Sphingolipid metabolism is dysregulated in PD.[25] In our study, the analysis with high-resolution LC-MS/MS revealed that the relative levels of S1P in the CSF of PD patients were 16 times higher than in control individuals, whereas sphingosine levels were significantly reduced. Previous studies reported the decreased plasma S1P levels in PD patients.[32,37] This observation contrasts with findings in Alzheimer's disease, where brain sphingosine levels were elevated, and S1P levels were diminished.[49] In contrast, ceramide levels were elevated in the plasma of PD patients[50] but reduced in the anterior cingulate cortex.[51] In addition, ceramide levels were increased in both plasma and CSF in multiple sclerosis.[52,53] These findings highlight the compartmentalized nature of sphingolipid metabolism across different neurodegenerative diseases and tissue layers, underscoring its potential role in disease-specific pathophysiological mechanisms.

Multiple lines of evidence indicate that endothelial Spns2-Mfsd2-mediated S1P export is essential for blood–brain barrier (BBB) maintenance[54] and is downregulated under inflammatory conditions,[55] while clinical biofluid studies support barrier dysfunction in PD.[56,57] Physiologically, there is a pronounced S1P gradient across the blood–brain/CSF barriers.[58] Impaired BBB integrity may contribute to increased S1P in CSF. In addition, our findings indicated that pathological α-syn enhanced both the activity and expression of microglial SPHK1, further supporting the elevation of S1P levels in the context of PD. In blood, S1P is derived primarily from erythrocytes and platelets and from vascular endothelium, and circulates bound to HDL–ApoM or albumin.[59] Multiple cohorts indicated that, the peripheral supply and carrier systems—such as HDL and its major apolipoprotein apoA-I—are impaired in

PD patients.[60,61] This likely contributes to the reduced plasma S1P levels.

The two sphingosine kinases exert opposing functions in the regulation of inflammation. SPHK1 is predominantly cytosolic, and the S1P it generates serves as an essential cofactor for the E3 ubiquitin ligase TRAF2, facilitating the cascade of events required for NF-κB nuclear translocation and thereby amplifying pro-inflammatory signaling.[42] Consequently, the overall action of SPHK1 is pro-inflammatory, as demonstrated in contexts such as colitis-associated tumorigenesis, endoplasmic reticulum stress, and arthritis.[62–64] By contrast, SPHK2 is primarily localized to several organelles,[65] including the nucleus, where the SPHK2–nuclear S1P axis directly inhibits HDAC1, promoting KLF4 acetylation at the epigenetic level and driving microglial polarization from a pro-inflammatory to an anti-inflammatory phenotype.[66] Pharmacological inhibition of SPHK2 disrupts this axis, impairs anti-inflammatory polarization, and exacerbates inflammatory responses.[66] These effects are consistent with a nuclear localization–dependent epigenetic mechanism for SPHK2.[67] Similarly, SPHK2 silencing with a specific siRNA or genetic deletion (*Sphk2*−/−) in mouse peritoneal macrophages leads to elevated production of inflammatory cytokines.[68] Our findings revealed a distinction in the transcriptional regulation of the genes encoding SPHK1 and SPHK2 during α-synuclein-driven neurodegeneration. In both hA53T transgenic mice and post-mortem PD patient brains, *Sphk1*/*SPHK1* expression was selectively upregulated in the substantia nigra, while *Sphk2*/*SPHK2* expression remained unaltered. Notably, *SPHK1* expression was strongly correlated with inflammatory gene transcription, whereas *SPHK2* was weakly correlated; inhibition of SPHK1 but not SPHK2 significantly reduced α-syn PFFs–induced NF-κB activation and TNFα elevation. In summary, SPHK1 rather than SPHK2 is selectively upregulated and closely associated with neuroinflammation during α-syn–driven neurodegeneration.

Across flies, mice, and humans, the two enzymes that catalyze S1P production are highly enriched in specific glial subpopulations.[39–41] This indicates that S1P is produced in glia but not in neurons. A lipidomic study with brain-region– and cell-type–resolution further reported that sphingolipid metabolism is markedly enriched in microglia,[69] thereby underscoring the central role of the microglial SPHK1/S1P axis in regulating neuroinflammation compared with neurons and astrocytes. In this study, α-syn PFFs induced *Sphk1* expression exclusively in microglia, while suppressing it in neurons and leaving astrocytes unaffected. Knockdown of microglial *Sphk1* in striatum significantly reduced neuroinflammation and the amount of pathological α-synuclein. These cell type-specific responses underscore microglia's central role in propagating S1P-dependent neuroinflammation and α-syn pathology. Consistently, either the catalytically inactive SPHK1 mutant (D81A) or *Sphk1* knockdown in microglia suppressed α-syn PFFs-induced NF-κB activation and TNFα expression, and these inhibitory effects were reversed by supplementation with high concentrations of S1P. However, low concentrations of exogenous S1P failed to activate NF-κB in *Sphk1*-silenced cells, indicating that S1P functions through an intracellular mechanism rather than a paracrine receptor-mediated pathway. Microglia engulf exogenous α-synuclein fibrils through a repertoire of receptors,[14–19] their limited ability to degrade these fibrils leads to intracellular accumulation of α-synuclein and the initiation of inflammatory responses.[20] In this study, inhibition of microglial SPHK1 reduced microglia-driven neuroinflammation and consequently attenuated α-syn PFFs-induced pathological α-syn accumulation in dopaminergic neurons. Thus, hyperactivated SPHK1 could initiate a feedforward loop: α-synuclein fibrils induce microglia to generate a S1P-mediated pro-inflammatory microenvironment, promoting neuronal α-synuclein aggregation and extracellular release, which is thereafter engulfed by microglia.

Recent clinical trials of GLP-1 receptor agonists in PD have yielded divergent results. In early-stage patients, a phase II study of lixisenatide demonstrated attenuation of motor worsening over 12 months,[70] whereas a phase III trial of exenatide was overall negative.[71] Considering the consistently very low CSF exposure of these agents,[72,73] particularly the even poorer CNS penetrance of lixisenatide, these findings suggest that the potential efficacy is more likely mediated through peripheral–central signaling and systemic anti-inflammatory or metabolic effects rather than extensive brain penetration. Previous work has shown that chronic administration of the selective SPHK1 inhibitor PF543 can modulate peripheral immunity: in sickle cell disease mice expressing human hemoglobin, four weeks of continuous PF543 treatment reduced erythrocyte SPHK1 activity and plasma S1P levels, accompanied by decreases in peripheral leukocyte counts, including both lymphocytes and neutrophils.[74] Clinically, a multicenter longitudinal study in drug-naïve early PD patients reported that higher neutrophil counts were associated with motor symptom worsening and reduced striatal DAT binding.[75] These observations raise the possibility that peripheral immunomodulation by PF543 may be clinically relevant. Our own exploratory data further demonstrate that PF543 is capable of crossing the BBB and reducing brain S1P concentrations, indicating a potential for direct central actions. However, the relative contributions of peripheral immune modulation versus central SPHK1 inhibition to the improvement of PD phenotypes remain unclear. Defining the balance between these mechanisms during chronic PF543 treatment will be critical to fully understand its therapeutic potential in PD.

In summary, this study demonstrates a robust elevation of S1P in CSF from PD patients, accompanied by reduced sphingosine levels. Consistently, elevated S1P is also detected in the striatum and midbrain of α-syn PFF-induced PD mice, with *Sphk1* showing the strongest upregulation among sphingolipid metabolic genes. Mechanistically, pathological α-syn selectively upregulates and activates SPHK1 in microglia, driving S1P-mediated NF-κB signaling and microglial activation. Genetic knockdown of *Sphk1* or pharmacological inhibition with PF543 attenuates neurodegeneration and PD-like neuropathology in mouse models, establishing S1P/SPHK1 as a potential therapeutic target to counteract PD and related synucleinopathies.

REFERENCES

1. Bloem B.R., Okun M.S. and Klein C. (2021). Parkinson's disease. *The Lancet* **397**:2284–2303. DOI:10.1016/S0140-6736(21)00218-X
2. Dorsey E.R., Sherer T., Okun M.S., et al. (2018). The emerging evidence of the Parkinson pandemic. *J. Parkinson's Dis.* **8**:S3–S8. DOI:10.3233/JPD-181474
3. Kalia L.V. and Lang A.E. (2015). Parkinson's disease. *The Lancet* **386**:896–912. DOI:10.1016/S0140-6736(14)61393-3
4. Bartels T., De Schepper S. and Hong S. (2020). Microglia modulate neurodegeneration in Alzheimer's and Parkinson's diseases. *Science* **370**:66–69. DOI:10.1126/science.abb8587
5. Hickman S., Izzy S., Sen P., et al. (2018). Microglia in neurodegeneration. *Nat. Neurosci.* **21**:1359–1369. DOI:10.1038/s41593-018-0242-x
6. Booms A., Pierce S.E., van der Schans E.J.C., et al. (2024). Parkinson's disease risk enhancers in microglia. *iScience* **27**:DOI:10.1016/j.isci.2024.108921
7. Gosselin D., Skola D., Coufal N.G., et al. (2017). An environment-dependent transcriptional network specifies human microglia identity. *Science* **356**:eaal3222. DOI:10.1126/science.aal3222
8. Nott A., Holtman I.R., Coufal N.G., et al. (2019). Brain cell type–specific enhancer–promoter interactome maps and disease-risk association. *Science* **366**:1134–1139. DOI:10.1126/science.aay0793
9. Prinz M., Jung S. and Priller J. (2019). Microglia biology: One century of evolving concepts. *Cell* **179**:292–311. DOI:10.1016/j.cell.2019.08.053
10. Liddelow S.A., Guttenplan K.A., Clarke L.E., et al. (2017). Neurotoxic reactive astrocytes are induced by activated microglia. *Nature* **541**:481–487. DOI:10.1038/nature21029
11. Dickson D.W. (2012). Parkinson's disease and parkinsonism: Neuropathology. *Cold Spring Harb. Perspect. Med.* **2**:a009258. DOI:10.1101/cshperspect.a009258
12. Tanriöver G., Bacioglu M., Schweighauser M., et al. (2020). Prominent microglial inclusions in transgenic mouse models of α-synucleinopathy that are distinct from neuronal lesions. *Acta Neuropathol. Commun.* **8**:133. DOI:10.1186/s40478-020-00993-8
13. Lee H.J., Bae E.J. and Lee S.J. (2014). Extracellular α-synuclein—A novel and crucial factor in Lewy body diseases. *Nat. Rev. Neurol.* **10**:92–98. DOI:10.1038/nrneurol.2013.275
14. Xiong M., Xia D., Yu H., et al. (2024). Microglia process α - synuclein fibrils and enhance their pathogenicity in a TREM2 - dependent manner. *Adv. Sci.* **12**:e2413451. DOI:10.1002/advs.202413451
15. Panicker N., Sarkar S., Harischandra D.S., et al. (2019). Fyn kinase regulates misfolded α-synuclein uptake and NLRP3 inflammasome activation in microglia. *J. Exp. Med.* **216**:1411–1430. DOI:10.1084/jem.20182191
16. Long H., Zhang S., Zeng S., et al. (2022). Interaction of RAGE with α-synuclein fibrils mediates inflammatory response of microglia. *Cell Rep.* **40**:111401. DOI:10.1016/j.celrep.2022.111401
17. Mao X., Ou M.T., Karuppagounder S.S., et al. (2016). Pathological α-synuclein transmission initiated by binding lymphocyte-activation gene 3. *Science* **353**:aah3374. DOI:10.1126/science.aah3374
18. Zhang S., Liu Y.Q., Jia C., et al. (2021). Mechanistic basis for receptor-mediated pathological α-synuclein fibril cell-to-cell transmission in Parkinson's disease. *Proc. Natl. Acad. Sci. USA* **118**:e2011196118. DOI:10.1073/pnas.2011196118

19. Saunders A., Macosko E.Z., Wysoker A., et al. (2018). Molecular diversity and specializations among the cells of the adult mouse brain. *Cell* **174**:1015–1030.e16. DOI:10.1016/j.cell.2018.07.028
20. Scheiblich H., Dansokho C., Mercan D., et al. (2021). Microglia jointly degrade fibrillar alpha-synuclein cargo by distribution through tunneling nanotubes. *Cell* **184**:5089–5106.e21. DOI:10.1016/j.cell.2021.09.007
21. Alaamery M., Albesher N., Aljawini N., et al. (2021). Role of sphingolipid metabolism in neurodegeneration. *J. Neurochem.* **158**:25–35. DOI:10.1111/jnc.15044
22. Várkonyi J., Rosenbaum H., Baumann N., et al. (2003). Gaucher disease associated with parkinsonism: Four further case reports. *Am J. M. Genet. A* **116A**:348–351. DOI:10.1002/ajmg.a.10028
23. Robak L.A., Jansen I.E., van Rooij J., et al. (2017). Excessive burden of lysosomal storage disorder gene variants in Parkinson's disease. *Brain* **140**:3191–3203. DOI:10.1093/brain/awx285
24. Maceyka M. and Spiegel, S. (2014). Sphingolipid metabolites in inflammatory disease. *Nature* **510**:58–67. DOI:10.1038/nature13475
25. Cartier A. and Hla, T. (2019). Sphingosine 1-phosphate: Lipid signaling in pathology and therapy. *Science* **366**:eaar5551. DOI:10.1126/science.aar5551
26. Chao C.C., Gutiérrez-Vázquez C., Rothhammer V., et al. (2019). Metabolic control of astrocyte pathogenic activity via cPLA2-MAVS. *Cell* **179**:1483–1498.e22. DOI:10.1016/j.cell.2019.11.016
27. Mayo L., Trauger S.A., Blain M., et al. (2014). Regulation of astrocyte activation by glycolipids drives chronic CNS inflammation. *Nat. Med.* **20**:1147–1156. DOI:10.1038/nm.3681
28. Lee M.J., Thangada S., Claffey K.P., et al. (1999). Vascular endothelial cell adherens junction assembly and morphogenesis induced by sphingosine-1-phosphate. *Cell* **99**:301–312. DOI:10.1016/S0092-8674(00)81661-X
29. Mizugishi K., Yamashita T., Olivera A., et al. (2005). Essential role for sphingosine kinases in neural and vascular development. *Mol. Cell Biol.* **25**:11113–11121. DOI:10.1128/MCB.25.24.11113-11121.2005
30. Mitroi D.N., Deutschmann A.U., Raucamp M., et al. (2016). Sphingosine 1-phosphate lyase ablation disrupts presynaptic architecture and function via an ubiquitin-proteasome mediated mechanism. *Sci. Rep.* **6**:37064. DOI:10.1038/srep37064
31. Atkinson D., Nikodinovic Glumac J., Asselbergh B., et al. (2017). Sphingosine 1-phosphate lyase deficiency causes Charcot-Marie-Tooth neuropathy. *Neurology* **88**:533–542. DOI:10.1212/WNL.0000000000003595
32. Schwedhelm E., Englisch C., Niemann L., et al. (2021). Sphingosine-1-phosphate, motor severity, and progression in Parkinson's disease (MARK-PD). *Mov. Disord.* **36**:2178–2182. DOI:10.1002/mds.28652
33. Bonnaud S., Niaudet C., Legoux F., et al. (2010). Sphingosine-1-phosphate activates the AKT pathway to protect small intestines from radiation-induced endothelial apoptosis. *Cancer Res.* **70**:9905–9915. DOI:10.1158/0008-5472.CAN-10-2043
34. Morales-Ruiz M., Lee M.J., Zöllner S., et al. (2001). Sphingosine 1-Phosphate activates AKT, nitric oxide production, and chemotaxis through a Gi protein/phosphoinositide 3-kinase pathway in endothelial cells. *J. Biol. Chem.* **276**:19672–19677. DOI:10.1074/jbc.M009993200
35. Heras-Sandoval D., Pérez-Rojas J.M., Hernández-Damián J., et al. (2014). The role of PI3K/AKT/mTOR pathway in the modulation of autophagy and the clearance of protein aggregates in neurodegeneration. *Cell. Signal.* **26**:2694–2701. DOI:10.1016/j.cellsig.2014.08.019
36. Zheng Z., Zong Y., Ma Y., et al. (2024). Glucagon-like peptide-1 receptor: Mechanisms and advances in therapy. *Sig. Transduct. Target. Ther.* **9**:234. DOI:10.1038/s41392-024-01931-z
37. Wang X., Wang B., Ji F., et al. (2024). Discovery of plasma biomarkers for Parkinson's disease diagnoses based on metabolomics and lipidomics. *Chin. Chem. Lett.* **35**:109653. DOI:10.1016/j.cclet.2024.109653
38. Lee M.K., Stirling W., Xu Y., et al. (2002). Human α-synuclein-harboring familial Parkinson's disease-linked Ala-53 → Thr mutation causes neurodegenerative disease with α-synuclein aggregation in transgenic mice. *Proc. Natl. Acad. Sci. USA* **99**:8968–8973. DOI:10.1073/pnas.132197599
39. Chung H., Ye Q., Park Y.J., et al. (2023). Very-long-chain fatty acids induce glial-derived sphingosine-1-phosphate synthesis, secretion, and neuroinflammation. *Cell Metab.* **35**:855–874.e5. DOI:10.1016/j.cmet.2023.03.022
40. Bennett M.L., Bennett F.C., Liddelow S.A., et al. (2016). New tools for studying microglia in the mouse and human CNS. *Proc. Natl. Acad. Sci. USA* **113**:E1738–46. DOI:10.1073/pnas.1525528113
41. Li Q., Cheng Z., Zhou L., et al. (2019). Developmental heterogeneity of microglia and brain myeloid cells revealed by deep single-cell rna sequencing. *Neuron* **101**:207–223.e10. DOI:10.1016/j.neuron.2018.12.006
42. Alvarez S.E., Harikumar K.B., Hait N.C., et al. (2010). Sphingosine-1-phosphate is a missing cofactor for the E3 ubiquitin ligase TRAF2. *Nature* **465**:1084–1088. DOI:10.1038/nature09128
43. Wang Z., Min X., Xiao S.H., et al. (2013). Molecular basis of sphingosine kinase 1 substrate recognition and catalysis. *Structure* **21**:798–809. DOI:10.1016/j.str.2013.02.025
44. Rothhammer V., Borucki D.M., Tjon E.C., et al. (2018). Microglial control of astrocytes in response to microbial metabolites. *Nature* **557**:724–728. DOI:10.1038/s41586-018-0119-x
45. Schnute M.E., McReynolds M.D., Carroll J., et al. (2017). Discovery of a potent and selective sphingosine kinase 1 inhibitor through the molecular combination of chemotype-distinct screening hits. *J. Med. Chem.* **60**:2562–2572. DOI:10.1021/acs.jmedchem.7b00070
46. Yun S.P., Kam T.I., Panicker N., et al. (2018). Block of A1 astrocyte conversion by microglia is neuroprotective in models of Parkinson's disease. *Nat. Med.* **24**:931–938. DOI:10.1038/s41591-018-0051-5
47. Luk K.C., Kehm V., Carroll J., et al. (2012). Pathological α-synuclein transmission initiates parkinson-like neurodegeneration in nontransgenic mice. *Science* **338**:949–953. DOI:10.1126/science.1227157
48. Liu J., Xu Y., Ji Y., et al. (2023). Sustained microglial activation and accelerated elimination of dendritic spines during acute sleep deprivation and restoration. *The Innovation Life* **1**:100037. DOI:10.59717/j.xinn-life.2023.100037
49. He X., Huang Y., Li B., et al. (2010). Deregulation of sphingolipid metabolism in Alzheimer's disease. *Neurobiol. Aging* **31**:398–408. DOI:10.1016/j.neurobiolaging.2008.05.010
50. Mielke M.M., Maetzler W., Haughey N.J., et al. (2013). Plasma ceramide and glucosylceramide metabolism is altered in sporadic Parkinson's disease and associated with cognitive impairment: A pilot study. *PLoS One* **8**:e73094. DOI:10.1371/journal.pone.0073094
51. Abbott S.K., Li H., Muñoz S.S., et al. (2014). Altered ceramide acyl chain length and ceramide synthase gene expression in Parkinson's disease. *Mov. Disord.* **29**:518–526. DOI:10.1002/mds.25729
52. Filippatou A.G., Moniruzzaman M., Sotirchos E.S., et al. (2021). Serum ceramide levels are altered in multiple sclerosis. *Mult. Scler.* **27**:1506–1519. DOI:10.1177/1352458520971816
53. Vidaurre O.G., Haines J.D., Katz Sand I., et al. (2014). Cerebrospinal fluid ceramides from patients with multiple sclerosis impair neuronal bioenergetics. *Brain* **137**:2271–2286. DOI:10.1093/brain/awu139
54. Wang Z., Zheng Y., Wang F., et al. (2020). Mfsd2a and Spns2 are essential for sphingosine-1-phosphate transport in the formation and maintenance of the blood-brain barrier. *Sci. Adv.* **6**:eaay8627. DOI:10.1126/sciadv.aay8627
55. Jeya Paul J., Weigel C., Müller T., et al. (2020). Inflammatory conditions disrupt constitutive endothelial cell barrier stabilization by alleviating autonomous secretion of sphingosine 1-phosphate. *Cells* **9**:928. DOI:10.3390/cells9040928
56. Pisani V., Stefani A., Pierantozzi M., et al. (2012). Increased blood-cerebrospinal fluid transfer of albumin in advanced Parkinson's disease. *J. Neuroinflammation* **9**:670. DOI:10.1186/1742-2094-9-188
57. Janelidze S., Hertze J., Nägga K., et al. (2017). Increased blood-brain barrier permeability is associated with dementia and diabetes but not amyloid pathology or APOE genotype. *Neurobiol. Aging* **51**:104–112. DOI:10.1016/j.neurobiolaging.2016.11.017
58. Männer A., Thomas D., Wagner M., et al. (2020). Sphingosine 1-phosphate levels in cerebrospinal fluid after subarachnoid hemorrhage. *Neurol. Res. Pract.* **2**:49. DOI:10.1186/s42466-020-00093-x
59. Christoffersen C., Obinata H., Kumaraswamy S.B., et al. (2011). Endothelium-protective sphingosine-1-phosphate provided by HDL-associated apolipoprotein M. *Proc. Natl. Acad. Sci. USA* **108**:9613–9618. 10.1073/pnas.1103187108
60. Choe C., Petersen E., Lezius S., et al. (2021). Association of lipid levels with motor and cognitive function and decline in advanced Parkinson's disease in the Mark-PD study. *Parkinsonism Relat. Disord.* **85**:5–10. DOI:10.1016/j.parkreldis.2021.02.007
61. Qiang J.K., Wong Y.C., Siderowf A., et al. (2013). Plasma apolipoprotein A1 as a biomarker for Parkinson disease. *Ann. Neurol.* **74**:119–127. DOI:10.1002/ana.23872
62. Liang J., Nagahashi M., Kim E.Y., et al. (2013). Sphingosine-1-phosphate links persistent STAT3 activation, chronic intestinal inflammation, and development of colitis-associated cancer. *Cancer Cell* **23**:107–120. DOI:10.1016/j.ccr.2012.11.013
63. Park K., Ikushiro H., Seo H.S., et al. (2016). ER stress stimulates production of the key antimicrobial peptide, cathelicidin, by forming a previously unidentified intracellular S1P signaling complex. *Proc. Natl. Acad. Sci. USA* **113**:E1334–42. DOI:10.1073/pnas.1504555113
64. Baker D.A., Barth J., Chang R., et al. (2010). Genetic sphingosine kinase 1 deficiency significantly decreases synovial inflammation and joint erosions in murine TNF-α–induced arthritis. *J. Immunol.* **185**:2570–2579. DOI:10.4049/jimmunol.1000644
65. Kunkel G.T., Maceyka M., Milstien S., et al. (2013). Targeting the sphingosine-1-phosphate axis in cancer, inflammation and beyond. *Nat. Rev. Drug Discov.* **12**:688–702. DOI:10.1038/nrd4099
66. Ji J., Wang J., Yang J., et al. (2019). The intra-nuclear SphK2-S1P axis facilitates M1-to-M2 shift of microglia via suppressing HDAC1-mediated KLF4 deacetylation. *Front. Immunol.* **10**:1241. DOI:10.3389/fimmu.2019.01241
67. Hait N.C., Allegood J., Maceyka M., et al. (2009). Regulation of histone acetylation in the nucleus by sphingosine-1-phosphate. *Science* **325**:1254–1257. DOI:10.1126/science.1176709
68. Weigert A., Von Knethen A., Thomas D., et al. (2019). Sphingosine kinase 2 is a negative regulator of inflammatory macrophage activation. *Biochim. Biophys. Acta Mol. Cell Biol. Lipids* **1864**:1235–1246. DOI:10.1016/j.bbalip.2019.05.008
69. Fitzner D., Bader J.M., Penkert H., et al. (2020). Cell-type- and brain-region-resolved mouse brain lipidome. *Cell Rep.* **32**:108132. DOI:10.1016/j.celrep.2020.108132
70. Meissner W.G., Remy P., Giordana C., et al. (2024). Trial of lixisenatide in early

Parkinson's disease. *N. Engl. J. Med.* **390**:1176–1185. DOI:10.1056/NEJMoa2312323
71. Vijiaratnam N., Girges C., Auld G., et al. (2025). Exenatide once a week versus placebo as a potential disease-modifying treatment for people with Parkinson's disease in the UK: A phase 3, multicentre, double-blind, parallel-group, randomised, placebo-controlled trial. *The Lancet* **405**:627–636. DOI:10.1016/S0140-6736(24)02808-3
72. Athauda D., Maclagan K., Skene S.S., et al. (2017). Exenatide once weekly versus placebo in Parkinson's disease: a randomised, double-blind, placebo-controlled trial. *The Lancet* **390**:1664–1675. DOI:10.1016/S0140-6736(17)31585-4
73. Christensen M., Sparre-Ulrich A.H., Hartmann B., et al. (2015). Transfer of liraglutide from blood to cerebrospinal fluid is minimal in patients with type 2 diabetes. *Int. J. Obes.* **39**:1651–1654. DOI:10.1038/ijo.2015.136
74. Zhang Y., Berka V., Song A., et al. (2014). Elevated sphingosine-1-phosphate promotes sickling and sickle cell disease progression. *J. Clin. Invest.* **124**:2750–2761. DOI:10.1172/JCI74604
75. Kim R., Kang N., Byun K., et al. (2023). Prognostic significance of peripheral neutrophils and lymphocytes in early untreated Parkinson's disease: An 8-year follow-up study. *J. Neurol. Neurosurg. Psychiatry.* **94**:1040–1046. DOI:10.1136/jnnp-2022-330394

FUNDING AND ACKNOWLEDGMENTS

We acknowledge the original authors of the datasets for their valuable contributions to this research (GSE26927, GSE152100, GSE11574, STDS0000021). We thank Yaping Yan from the College of Life Science at Shaanxi Normal University for providing the pLenti-CD11b-mir30-shRNA vector. We thank Jie Yan, Ji Xu, and Jing ji from the First Affiliated Hospital of Shenzhen University for their assistance in human sample collection. We thank Lei Guo from the Interdisciplinary Institute of Medical Engineering at Fuzhou University for his technical support. The graphical abstract, fig 3H, and fig S8A were created with BioRender.com. This work was supported by Hong Kong Collaborative Research Fund (No. C2011-21GF). The funders had no role in study design, data collection and analysis, decision to publish, or preparation of the manuscript.

AUTHOR CONTRIBUTIONS

Conceptualization: J.F., X.W., and Z.C.; Methodology: J.F., X.W., and Z.C.; Investigation: J.F. and X.W.; Visualization: J.F. and X.W.; Resources: D.L., F.W., P.W., C.Y., F.J., D.Z., X.C., W.L., and M.L.; Funding acquisition: Z.C.; Project administration: Z.C.; Supervision: Z.C.; Writing – original draft: J.F. and X.W.; Writing – review & editing: J.F., X.W., S.H., X.S., and Z.C.. All authors contributed to the manuscript and approved the final version.

DECLARATION OF INTERESTS

Zongwei Cai is an Editorial Board member of The Innovation Life and was blinded from reviewing or making final decisions on the manuscript. Peer review was handled independently of this member and their research group. The authors (J.F., X.W., and Z.W.) have filed a US provisional patent related to this work (Application Number US 6369495563, filed on September 17, 2024). All other authors declare no conflicts of interest.

ETHICAL STATEMENT AND PATIENT CONSENT

The study involving human participants complied with ethical standards and was approved by the Medical Ethics Committee of Shenzhen Second People's Hospital, with informed consent obtained from all participants. All animal experimental procedures were conducted in accordance with the guidelines of Hong Kong Baptist University (HKBU) and approved by the HKBU Committee on the Use of Human and Animal Subjects in Teaching and Research.

DATA AND CODE AVAILABILITY

The processed transcriptomic datasets have been uploaded to Sequence Read Archive (NCBI BioProject: PRJNA1146572). This paper does not include any original code. Additional information necessary for reanalyzing the reported data is available upon request from the lead contact.

SUPPLEMENTAL INFORMATION

It can be found online at https://doi.org/10.59717/j.xinn-life.2025.100164

LEAD CONTACT WEBSITE

Zongwei Cai: https://person.eitech.edu.cn/lxb/czw/main.htm